

# 江西吉泰盆地梅岗地区上白垩统周田组沉积特征与沉积模式

余小灿<sup>1</sup>, 王春连<sup>2</sup>, 孟令阳<sup>3</sup>, 颜开<sup>2</sup>

(1. 中国地质科学院地质研究所, 北京 100037; 2. 中国地质科学院矿产资源研究所, 自然资源部成矿作用与资源评价重点实验室, 北京 100037; 3. 江西省地质局第五地质大队, 江西 新余 338000)

**摘要:** 江西吉泰盆地上白垩统周田组赋存丰富的卤水型锂资源, 其沉积演化与沉积模式尚存争议。本次工作在前人研究基础上, 通过对吉泰盆地梅岗地区5口钻孔岩芯的精细描述, 结合岩石学、矿物学和石膏硫同位素研究, 分析周田组岩性组合特征, 识别沉积相类型与沉积特征, 总结其沉积演化过程。根据岩性组合和沉积构造特征, 周田组地层可分为下部的滨-浅湖相和上部的盐湖相沉积。周田组沉积早期, 沉积中心位于盆地东南的泰和与宜春一带, 主要由砾岩、细砂岩、泥质粉砂岩和粉砂质泥岩组成; 湖盆边缘发育冲积-河流相, 向盆地内过渡为三角洲相, 至湖盆沉积中心为滨-浅湖相。周田组沉积晚期, 气候逐渐变干旱, 湖水不断蒸发形成了盐湖环境, 发育泥岩和石膏岩的韵律沉积, 表明湖水周期性咸化和淡化转化的沉积过程。石膏岩的 $\delta^{34}\text{S}$ 值为 $-6.0\text{\textperthousand}$ ~ $-15.4\text{\textperthousand}$ , 集中在 $-10.1\text{\textperthousand}$ ~ $-12.8\text{\textperthousand}$ 之间, 指示其形成于开放的成盐环境, 几乎未受到细菌还原作用的影响。梅岗地区含盐系地层向北西变厚, 裂隙储层发育, 显示了良好的卤水型锂矿找矿远景。

**关键词:** 沉积演化; 沉积模式; 盐湖; 硫同位素; 吉泰盆地

中图分类号: P575; P586; P611.4 文献标识码: A

文章编号: 1000-6524(2025)04-0788-15

## Sedimentary characteristics and depositional model of the Upper Cretaceous Zhou'tan Formation in the Meigang area of the Jitai Basin, Jiangxi Province

YU Xiao-can<sup>1</sup>, WANG Chun-lian<sup>2</sup>, MENG Ling-yang<sup>3</sup> and YAN Kai<sup>2</sup>

(1. Institute of Geology, Chinese Academy of Geological Sciences, Beijing 100037, China; 2. MNR Key Laboratory of Metallogeny and Mineral Assessment, Institute of Mineral Resources, Chinese Academy of Geological Sciences, Beijing 100037, China; 3. The Fifth Geological Brigade of Jiangxi Geological Bureau, Xinyu 338000, China)

**Abstract:** There are abundant brine-type lithium resources hosted in the Upper Cretaceous Zhou'tan Formation of the Jitai Basin, Jiangxi Province. However, its sedimentary evolution and depositional model remain controversial. On the basis of previous studies, through the detailed description of the cores of five boreholes in Meigang area of the Jitai Basin, combined with petrology, mineralogy and sulfur isotopes of gypsum, the lithofacies associations were analyzed, sedimentary facies types and sedimentary characteristics were identified, and the sedimentary evolutionary processes of the Zhou'tan Formation were summarized. According to the lithofacies associations and sedimentary structures, the sedimentary system of the Zhou'tan Formation can be divided into shore-shallow lake sedimentary system in the lower part and salt lake sedimentary system in the upper part. In the early deposition stage of

收稿日期: 2024-10-09; 接受日期: 2025-05-14; 编辑: 尹淑萍

基金项目: 中国地质科学院地质研究所基本科研业务费项目(J2315); 国家自然科学基金项目(U20A2092); 中央级公益性科研院所基本科研业务费专项(KK2005)

作者简介: 余小灿(1988- ), 男, 副研究员, 主要从事卤水型矿床及沉积学方向研究, E-mail: xiaocany1988@163.com; 通讯作者: 王春连(1983- ), 男, 研究员, 主要从事沉积矿床方向研究, E-mail: wangchunlian312@163.com。

the Zhoutian Formation, the depositional center was located between Taihe and Zhixia areas in the southeast basin, and was mainly composed of conglomerate, fine sandstone, muddy siltstone and silty mudstone. The alluvial-fluvial facies developed at the edge of the lake basin, transitioning to delta facies in the intra-basin, and to the sedimentary center of the lake basin, shore-shallow lake facies. In the late deposition period of the Zhoutian Formation, the climate gradually became arid, and a salt lake environment was formed by the continuous evaporation of the lake water. The rhythmic deposition of mudstone and gypsum rocks was developed, indicating the periodic salinization and desalination process of the lake water. The  $\delta^{34}\text{S}$  value of gypsum is of  $8.0\text{‰} \sim 15.4\text{‰}$ , mainly concentrated in the range of  $10.1\text{‰} \sim 12.8\text{‰}$ , indicating that the gypsum was formed in an open salt-forming environment, and almost unaffected by the bacterial reduction process. In the Meigang area, the salt-bearing strata thicken towards the northwest, with well-developed fractured reservoirs, presenting a promising prospect for lithium brine-type deposit exploration.

**Key words:** sedimentary evolution; depositional model; salt lake; sulfur isotope; Jitai Basin

**Fund support:** Basic Scientific Research Fund of the Institute of Geology, Chinese Academy of Geological Sciences (J2315); National Natural Science Foundation of China (U20A2092); Basic Scientific Research Fund of the China Central Non-Commercial Institute (KK2005)

第四纪陆相盐湖卤水或深部地下卤水常储藏着丰富的锂、钾、铷、铯等矿产资源(Warren, 2010; Munk *et al.*, 2016; 张西营等, 2016; Li *et al.*, 2019; Dugamin *et al.*, 2021)。全球卤水型锂资源主要分布在南美西部安第斯高原、美国西部高原和中国青藏高原地区,其中以南美“锂三角”地区的锂资源最为丰富,且品质较高(Munk *et al.*, 2016; López-Steinmetz *et al.*, 2020; López-Steinmetz and Salvi, 2021)。这些卤水型锂矿床形成于干旱气候条件下的封闭盐湖盆地环境(Bradley *et al.*, 2013; Munk *et al.*, 2016)。我国华南地区分布有晚白垩世至古近纪蒸发岩盆地,如江汉、衡阳、清江、吉泰、赣州、会昌、三水、南雄及苏北盆地等,也赋存丰富的盐类矿产和卤水资源(刘群等, 1987; 刘成林等, 2016; 余小灿等, 2022)。勘查结果显示,在江西吉泰盆地和赣州盆地上白垩统周田组含盐系地层中钻遇富锂卤水,最高含量超工业品位约4倍,镁锂比值( $<11$ )较低,是优质的卤水型锂矿(刘成林等, 2016; 周敏娟等, 2017; 廖达军等, 2019; 肖则佑等, 2023)。

吉泰盆地卤水型锂矿的形成与深部构造特征密切相关(刘志伟等, 2022),同时储卤地层的岩性特征及其沉积相展布对卤水运移和储存起重要控制作用。因此,对含盐系地层岩相特征分析和沉积模式研究,有利于预测储层的空间展布,对指导卤水型锂矿勘查具有重要意义。基于元素地球化学、储层矿物学、多同位素示踪以及水岩反应实验模拟,前人对吉泰盆地富锂卤水矿床的物质来源和富集过程主要有3种认识:①火成岩风化或深部物质的补给作用

(刘成林等, 2016; 周敏娟等, 2017; 廖达军等, 2019; 王春连等, 2020; 朱明波等, 2022);②原生水的蒸发浓缩作用(罗辉平等, 2018);③卤水与储层岩石间的水岩反应(马厚明等, 2021; Yu *et al.*, 2022)。目前,仅对吉泰盆地沉积特征和沉积环境做出初步研究(廖瑞君, 2000; 肖凯等, 2022),而对卤水储层的沉积特征和沉积演化认识不清,制约了富锂卤水矿床研究。因此,本文以吉泰盆地梅岗矿区5口钻孔岩芯为研究对象,开展岩石学、矿物学和石膏硫同位素研究,对上白垩统周田组地层进行岩性分类,讨论不同岩性组合的沉积相类型,分析其空间分布特征及沉积演化,建立沉积模式,以期为富锂卤水矿床勘查提供地质参考。

## 1 区域地质背景

### 1.1 构造背景

晚白垩世时期,由于古太平洋板块向欧亚大陆的俯冲,华南板块发育一系列北东、北北东向分布的断陷盆地,同时伴随强烈的火山活动,在盆内或盆地周缘发育燕山期火成岩(图1)(Gilder *et al.*, 1991; Zhou and Li, 2000; Shu *et al.*, 2009)。此外,盆地内充填大量冲积、河流和湖相红层、蒸发岩以及风成沉积(江新胜等, 1996; 陈丕基, 1997; Jiang *et al.*, 2008; Yan *et al.*, 2011; Chen *et al.*, 2017; 王九一等, 2021; Yu *et al.*, 2021)。

吉泰盆地位于华夏板块北缘,是白垩纪断陷盆地,面积  $4\text{ 000 km}^2$ (余心起等, 2005)。盆地周缘主要

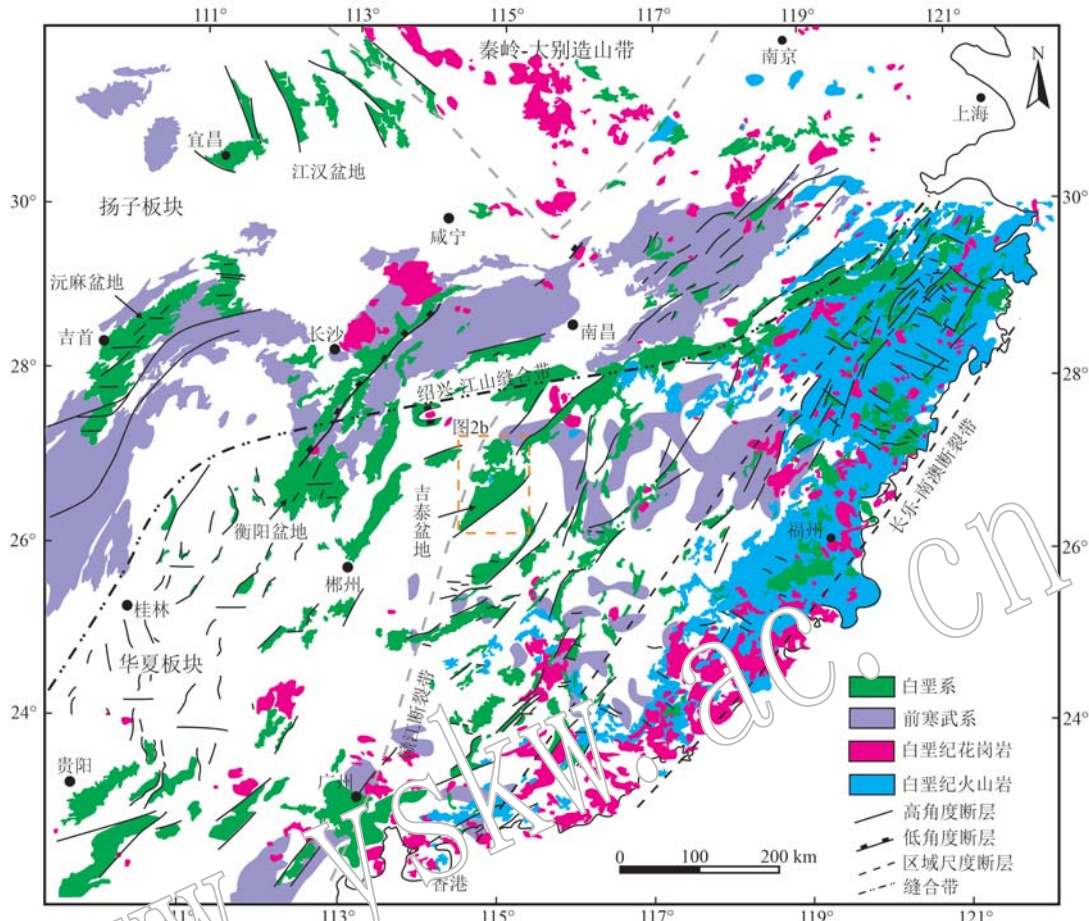


图1 华南白垩纪构造特征和火成岩分布(Li et al., 2014)

Fig. 1 Cretaceous tectonic feature and igneous rock distribution in South China (Li et al., 2014)

北东、北北向分布的断陷盆地是指图中北东向展布的白垩系沉积

the north-east and north-northwest trending fault basins refer to the north-east trending Cretaceous sediments shown in the figure

被赣江断裂、吉水断裂、永兴-峡江和遂川-德兴断裂控制。从北到南,盆内有吉安坳陷、早禾坳陷、高陂-梅岗隆起和泰和坳陷4个二级构造单元组成(图2a)(王春连等,2020;肖凯等,2022)。晚白垩世早期,受益缘遂川、吉水断裂的控制,泰和坳陷迅速扩张并大幅度下沉,北部沉降速度大于南部,沉积厚度呈现北厚南薄的特征;晚白垩世晚期,由于受到北东向断裂和盆地东、西缘断裂的控制,泰和坳陷的沉积、沉降中心向南迁移,形成了西南低、东北高的构造格局(肖凯等,2022)。

## 1.2 吉泰盆地地层

吉泰盆地前白垩系基底由新元古界至侏罗系组成,缺失奥陶系和志留系,主要由变质杂砂岩、板岩、碳酸盐岩和碎屑岩组成。盆地周缘大量出露加里东期和燕山期花岗岩(Zhou et al., 2006; Xu and Xu, 2015),而盆地内部零星出露白垩纪基性火成岩(彭

头平等,2004;余心起等,2005)。盆内充填的上白垩统是一套陆相沉积,从下至上可分为赣州群和圭峰群(江西省地质矿产局,1997)。从老到新,赣州群由茅店组和周田组组成,圭峰群分为河口组、塘边组和莲荷组(图2b)。茅店组由紫红色砂岩和杂色砾岩组成,局部夹玄武岩及中酸性凝灰岩。河口组岩性主要为棕红色砂岩和粉砂岩,夹紫红色含砾砂岩和泥岩,与下伏周田组地层整合接触。塘边组主要由砖红色砂岩、粉砂岩和砾岩组成。莲荷组岩性主要为棕红色砾岩、含砾砂岩和砂岩。其中,周田组是区内富含石膏的碎屑岩地层,与下伏茅店组地层整合接触,主要出露在盆地南缘的新圩、泰和及万合等地(图2b),主要由紫红色、青灰色泥岩、粉砂岩和薄层石膏岩组成,局部夹薄层细砂岩和砾岩。根据岩性组合特征,周田组地层从下至上可分为七段(马厚明等,2021):一段为杂色砾岩;二段为紫红色细

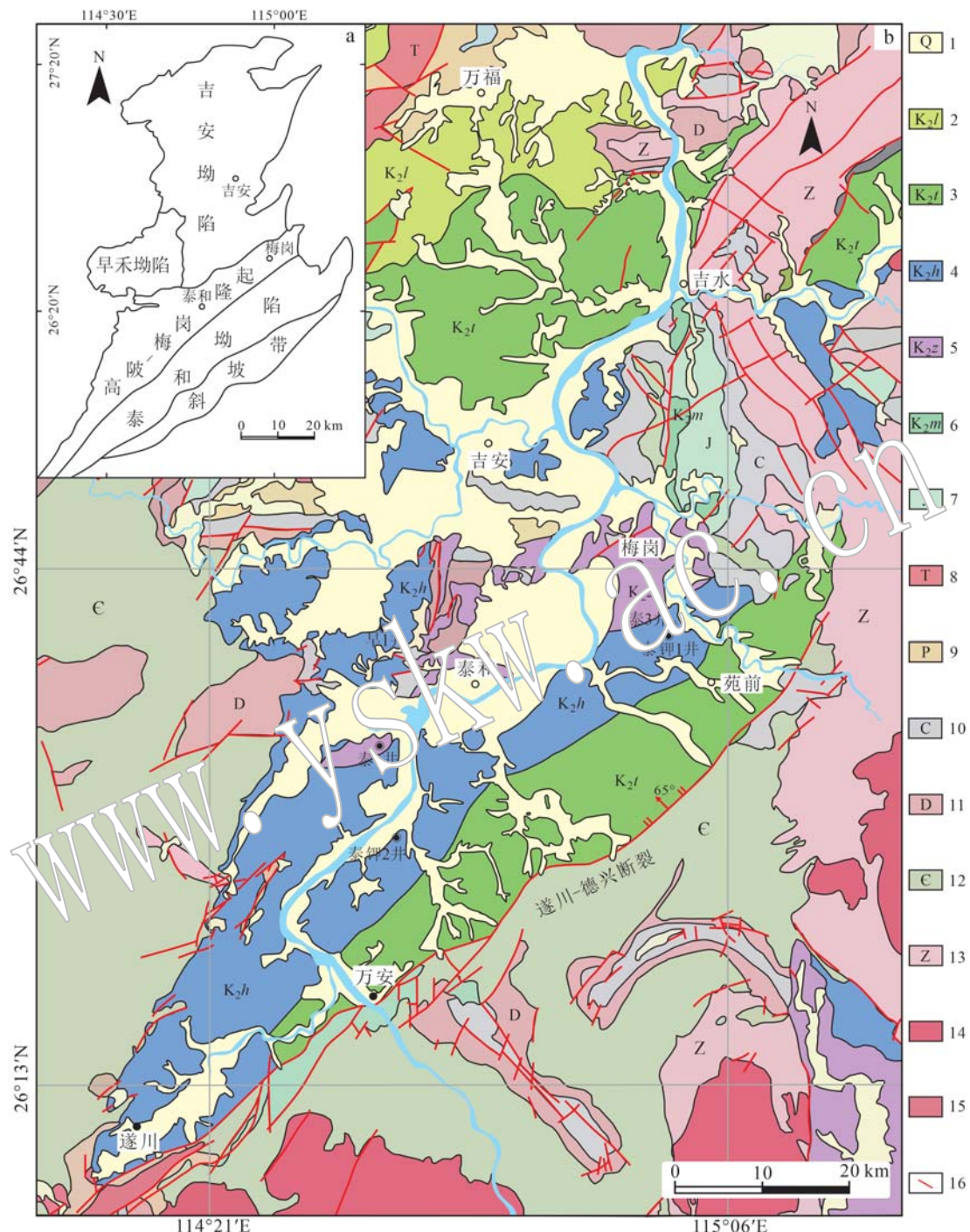


图 2 吉泰盆地构造区划(a)和地质图(b)(据肖凯等, 2022)

Fig. 2 Tectonic division (a) and geological map (b) of the Jitai Basin (after Xiao Kai et al., 2022)

1—第四系; 2—上白垩统莲荷组; 3—上白垩统塘边组; 4—上白垩统河口组; 5—上白垩统周田组; 6—上白垩统茅店组; 7—侏罗系;  
8—三叠系; 9—二叠系; 10—石炭系; 11—泥盆系; 12—寒武系; 13—震旦系; 14—燕山期花岗岩; 15—加里东期花岗岩; 16—断裂构造  
1—Quaternary; 2—Upper Cretaceous Lianhe Formation; 3—Upper Cretaceous Tangbian Formation; 4—Upper Cretaceous Hekou Formation;  
5—Upper Cretaceous Zhoutian Formation; 6—Upper Cretaceous Maodian Formation; 7—Jurassic; 8—Triassic; 9—Permian; 10—Carboniferous;  
11—Devonian; 12—Cambrian; 13—Sinian; 14—Yanshanian granite; 15—Caledonian granite; 16—fracture structure

砂岩和含砾砂岩; 三段为紫红色泥质粉砂岩、粉砂质泥岩、泥页岩, 夹薄层石膏岩, 泥岩中发育团块状、

脉状石膏; 四段为紫红色粉砂质泥岩、杂色泥页岩和泥灰岩, 夹薄层石膏岩, 泥岩中发育星点状、脉状

石膏；五段为紫红色粉砂质泥岩、泥页岩和泥灰岩，夹薄层石膏岩和红色凝灰岩，泥岩中发育星点状、脉状石膏；六段为紫红色复成分砾岩和含砾砂岩，夹砂岩；七段为紫红色细砂岩、粉砂岩、泥岩和杂色泥页岩，可见薄层石膏，泥岩中发育星点状石膏。富锂卤水主要赋存于第五段的构造破碎带及岩石孔隙和裂隙中(周敏娟等, 2017)。

## 2 样品采集与测试方法

### 2.1 样品采集

本次工作主要对梅岗矿区梅1井、2井、ZK8001、ZK8301、ZK8401共5个钻孔岩芯开展精细

描述(图3)。根据其岩性组合和沉积构造特征，分析并识别沉积相类型与特征。同时，采集代表性岩石样品，开展岩相学分析，结合扫描电镜能谱和X射线衍射分析，定性和半定量岩石矿物组合特征。另外，采集了28件石膏样品，用于硫同位素组成的测试分析。

### 2.2 测试方法

扫描电镜能谱分析在中国地质科学院地质研究所大陆动力学实验室完成。扫描电子显微镜型号为FEI NOVA NanoSEM 450，能谱仪为OXFORD X-Max (50 mm<sup>2</sup>)，操作电压为20 kV。

X射线衍射分析在北京北达智汇微构造分析测试中心完成。仪器型号布鲁克D8 Advance衍射仪，

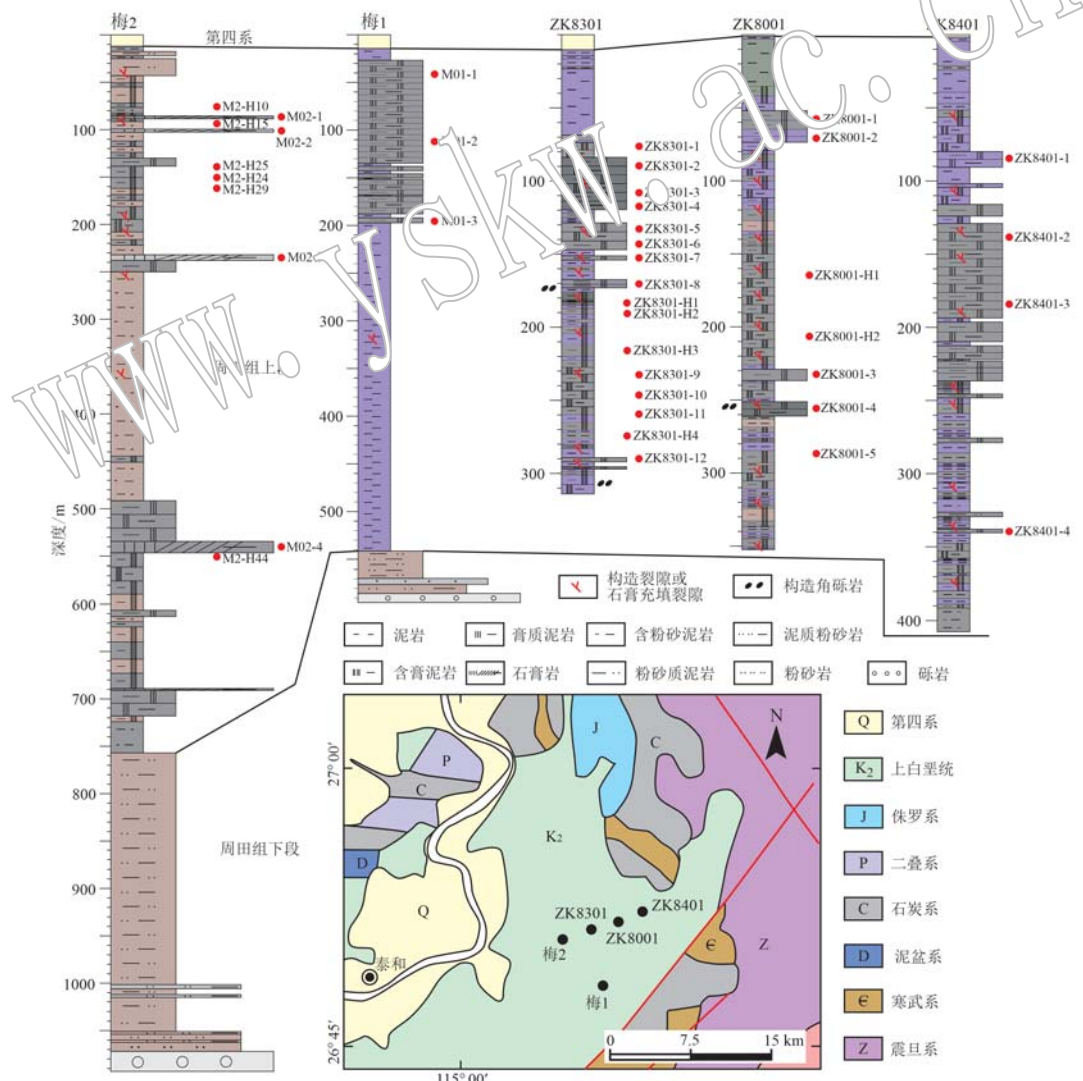


图3 吉泰盆地梅岗矿区钻孔岩芯柱状图

Fig. 3 Column diagram of drill cores in the Meigang area of the Jitai Basin

铜旋转靶工作电压40 kV,电流100 mA,波长 $1.5406\text{ \AA}$ ,连续扫描角度( $2\theta$ )为 $3^\circ\sim70^\circ$ ,速度为 $8^\circ/\text{min}$ ,步宽 $0.02^\circ$ 。原始数据运用JADE 6.5软件处理,具体程序见检测标准SY/T 5163-2018沉积岩黏土矿物和常见非黏土矿物X射线衍射分析方法。

在硫同位素测试前,首先对石膏样品进行X射线衍射分析,挑选出纯石膏样品。然后,用小刀刮掉表层不干净物质,用超声波清洗机清洗2次,低温烘干处理后破碎至200目。石膏硫同位素测试在核工业北京地质研究院测试中心完成。测试仪器为MAT251型质谱仪,分析精度为2‰。

### 3 结果

#### 3.1 岩相类型及特征

基于梅岗地区5口钻孔的岩芯描述、岩石薄片的显微镜下特征和全岩X射线衍射分析结果(图4),共识别出9种岩相类型。

(1) 颗粒支撑的砾岩(Gc)。颗粒支撑的块状砾岩(图5a),发育在周田组地层底部,厚度约 $10\sim20\text{ m}$ 。砾石成分为灰岩和方解石(图6a),大小 $0.2\sim9\text{ cm}$ ,棱角状至圆状,泥质或粉砂质杂基充填。这种岩石主要形成于高流速的冲积环境。

(2) 层状细砂岩(Sp)。灰白色、棕色极细至细粒砂岩,主要发育在周田组下部层位,厚度 $0.05\sim2.0\text{ m}$ 。可见平行层理、脉状层理、低角度交错层理和板状交错层理(图5b、5c),见泥屑和垂直层面虫迹(图5d)。这种岩石是水下高能量密度流快速沉积的结果。

(3) 波状、脉状泥质粉砂岩(Sw)。棕色、杂色泥质粉砂岩,厚度 $0.27\sim1.5\text{ m}$ 。发育脉状、波状层理(图5e、5f),可见虫迹(图5g),偶见水平或包卷层理(图5h)。这类岩石指示其形成于强、弱交替水动力条件。

(4) 块状粉砂质泥岩(Fsm)。棕色块状粉砂质泥岩,是主要的岩相类型之一,不发育层理构造,厚度 $0.4\sim3\text{ m}$ 。可见星点状、云朵状硬石膏及泄水构造(图5i)。该岩石是静水状态下悬浮颗粒缓慢沉降的结果。

(5) 块状泥岩(Fm)。棕红色块状泥岩,厚度 $0.15\sim45\text{ m}$ ,是主要的岩相类型之一。可见薄层状石膏岩互层(图5j),泥岩中可见星点状、脉状和团块

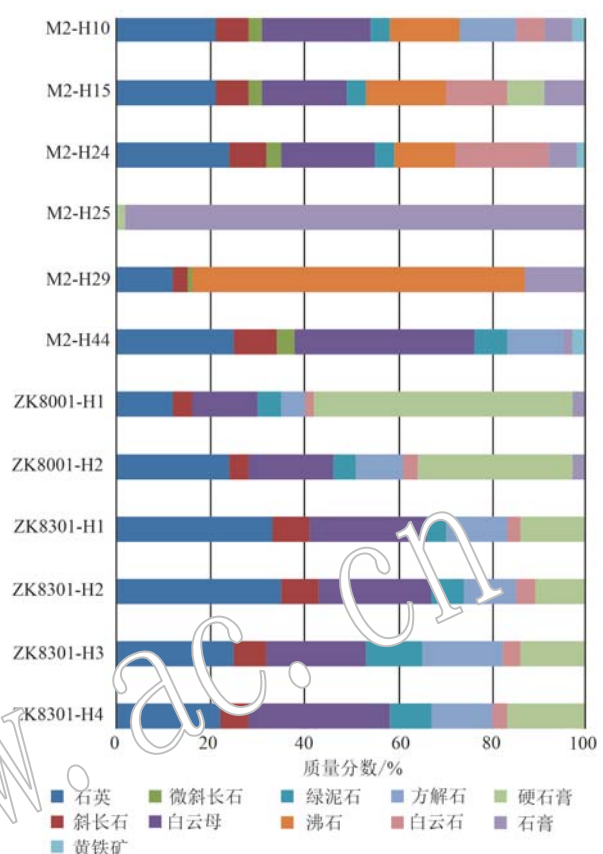


图4 吉泰盆地周田组代表性岩石矿物组合  
Fig. 4 Mineral assemblage of representative cores from the Zhoutian Formation of the Jitai Basin

状硬石膏(图5k)。该岩石是静水状态下悬浮颗粒缓慢沉降而成。

(6) 水平层理泥岩(Fh)。青灰色、棕褐色泥岩,水平层理发育,与薄层状石膏岩互层(图5l、5m),是发育最广泛的岩相类型之一,厚度 $0.2\sim35\text{ cm}$ 。可见粉砂粒级纹层,呈现明显的粒序层理(图6b),团块状硬石膏切穿层理或顺层理分布(图5o、5p、6c),可见贯穿层理的硬石膏脉及包卷层理(图5q、5r)。这类岩石指示了在较弱水动力条件下悬浮颗粒沉降形成的。

(7) 构造破碎角砾岩(Gm)。杂基支撑的块状砾岩(图5n),发育在周田组上部含石膏层段,厚度 $0.15\sim0.25\text{ m}$ 。砾石成分主要为棕褐色泥岩,棱角至次棱角状,方解石胶结(图5n和6d)。

(8) 薄层状石膏岩(Gp)。白色或透明石膏岩(图5j、5l、5m),厚度 $0.5\sim5\text{ cm}$ ,发育韵律条带状构造,是主要的岩相类型之一。镜下可见近乎垂直的两组解理(图6e)。该类岩石常形成于水体咸化的



图5 吉泰盆地周田组岩芯的典型沉积特征

Fig. 5 Typical sedimentary characteristics of cores from the Zhouyuan Formation of the Jitai Basin

a—块状砾岩(梅2井, 1 072.35 m); b—灰、灰白色细砂岩, 发育平行层理和低角度交错层理(梅2井, 1 021.35 m); c—灰白色细砂岩, 发育平行层理、板状交错层理和低角度交错层理(梅2井, 961.50 m); d—灰白色砂岩, 发育泥屑和虫迹(梅2井, 1 012.15 m); e—棕色脉状层理砂岩(梅2井, 927.25 m); f—棕色泥质粉砂岩, 发育脉状、波状层理(梅2井, 926.30 m); g—棕色泥质粉砂岩, 发育虫迹(梅2井, 926.30 m); h—棕色泥质粉砂岩, 出现水平和包卷层理(梅2井, 1 001.23 m); i—棕色块状粉砂质泥岩, 发育泄水构造(梅2井, 925.10 m); j—薄层石膏与棕色泥岩互层(ZK8001井, 42.01~51.04 m); k—棕色块状泥岩发育团块状硬石膏(梅2井, 945.50 m); l—薄层石膏与水平层理泥岩互层(ZK8301井, 290.85 m); m—薄层石膏与水平层理泥岩互层(梅2井, 89.95 m); n—构造破碎角砾岩(ZK8001井, 251.41 m); o—水平层理泥岩, 发育团块状硬石膏, 并切穿水平层理, 同时上、下部层理弯曲(ZK8301井, 289.28 m); p—水平层理泥岩, 团块状硬石膏顺层分布(ZK8401井, 48.50 m); q—切穿层理的硬石膏脉, 层理发生错动, 显示正断层特征(梅2井, 90.50 m); r—切穿层理的硬石膏脉及包卷层理(ZK8401井, 49.52 m)

a—massive conglomerate, Mei2 borehole, 1 072.35 m; b—grey fine sandstone with parallel bedding and low-angle cross-bedding, Mei2 borehole, 1 021.35 m; c—grey fine sandstone with parallel bedding and tabular and low-angle cross-bedding, Mei2 borehole, 961.50 m; d—grey sandstone with mud chips and burrows, Mei2 borehole, 1 012.15 m; e—brown sandstone with flaser bedding, Mei2 borehole, 927.25 m; f—brown muddy siltstone with flaser and wave bedding, Mei2 borehole, 926.30 m; g—brown muddy siltstone with burrows, Mei2 borehole, 926.30 m; h—brown muddy siltstone with horizontal and convolute bedding, Mei2 borehole, 1 001.23 m; i—brown silty mudstone with water-escape structure, Mei2 borehole, 925.10 m; j—interbedding of laminated gypsum and brown mudstone, ZK8001 borehole, 42.01~51.04 m; k—brown massive mudstone with crumby anhydrite, Mei2 borehole, 945.50 m; l—interbedding of laminated gypsum and horizontal bedded mudstone, ZK8301 borehole, 290.85 m; m—interbedded laminated gypsum and horizontal bedded mudstone, Mei2 borehole, 89.95 m; n—fault breccia, ZK8001 borehole, 251.41 m; o—horizontal bedded mudstone with crumby anhydrites, which cut through horizontal bedding and compress the upper and lower layers bended, ZK8301 borehole, 289.28 m; p—the nodular anhydrite is distributed within the horizontal bedded mudstone, ZK8401 borehole, 48.50 m; q—veined anhydrite cut through horizontal bedded mudstone with convolute bedding, ZK8401 borehole, 49.52 m

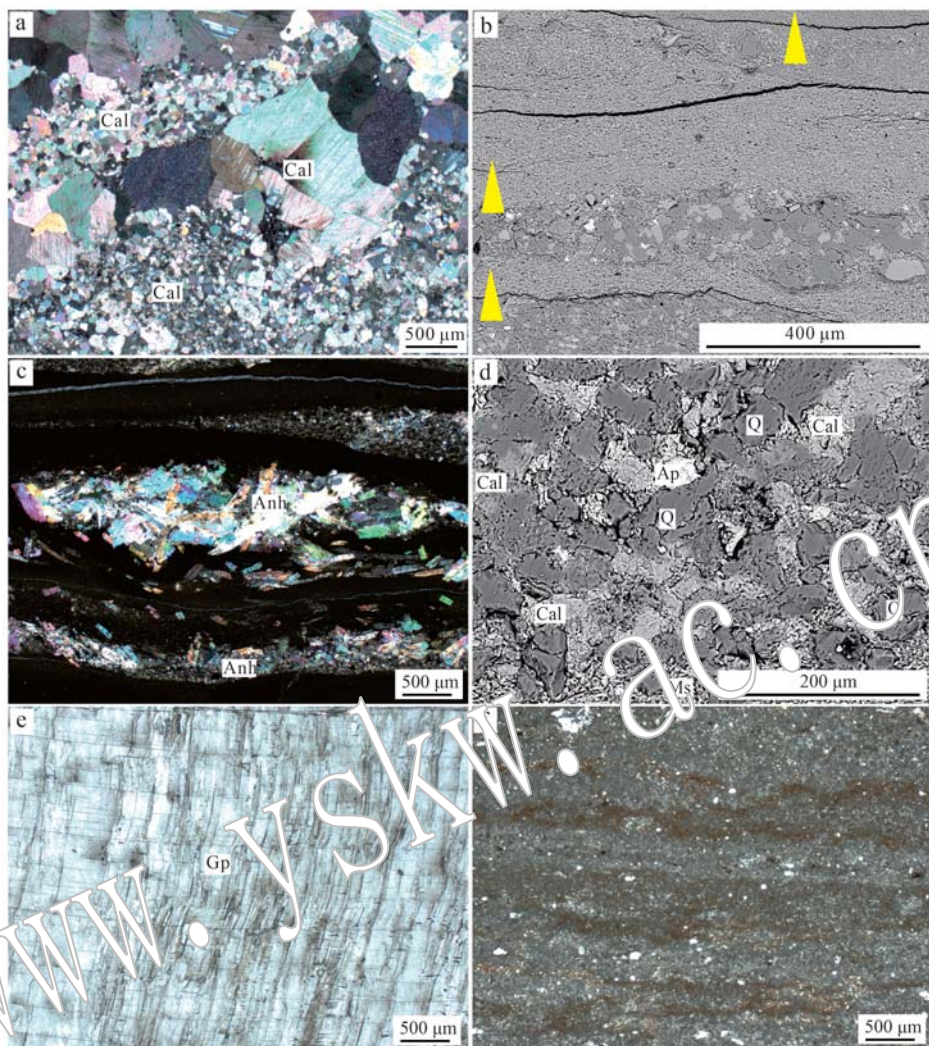


图 6 吉泰盆地周田组岩芯样品显微镜下特征

Fig. 6 Microphotographs of the core samples from the Zhouyuan Formation of the Jitai Basin

a—方解石砾石(正交偏光,梅2井,1 072.95 m); b—水平层理泥岩,粉砂纹层的出现呈现粒序层理(ZK8301井,290.85 m); c—泥岩中透镜状硬石膏顺层分布和切穿水平层理,上下部层理弯曲(正交偏光,梅2井,216.40 m); d—构造破碎角砾岩,方解石胶结(扫描电镜,ZK8001井,251.41 m); e—石膏发育近乎垂直的两组解理(正交偏光,梅2井,216.40 m); f—凝灰岩,可见黏土条带(梅2井,159.95 m); Cal—方解石; Q—石英; Ap—磷灰石; Anh—硬石膏; Gp—石膏

a—calcite gravel, cross-polarized light, Mei2 borehole, 1 072.95 m; b—horizontal bedded mudstone with graded bedding due to the presence of silty lamina, ZK8301 borehole, 290.85 m; c—the nodular anhydrite is distributed within the horizontal bedded mudstone, cut through horizontal bedding and compress the upper and lower layers bent, cross-polarized light, Mei2 borehole, 216.40 m; d—fault breccias, Mei2 borehole, 251.41 m; e—gypsum develops two nearly vertical cleavages, Mei2 borehole, 216.40 m; f—clay bands can be seen under the microscope in the tuff, Mei2 borehole, 159.95 m; Cal—calcite; Q—quartz; Ap—apatite; Anh—anhydrite; Gp—gypsum

蒸发盐湖环境。

(9) 块状凝灰岩。棕红色凝灰岩,厚度0.1~0.5 m,发育在梅2井112~168 m深度段,为火山灰堆积经成岩作用而成,可见黏土条带(图6f)。

### 3.2 沉积相类型及特征

根据不同岩相类型的组合及沉积建造特征,识

别并划分了3种沉积相类型,即滨湖相、浅湖相和盐湖相。肖凯等(2022)在吉泰盆地边缘识别出冲积-河流相和三角洲相沉积。

(1) 滨湖相。该沉积相主要有砾岩(Gc)、薄层细砂岩(Sp)和泥质粉砂岩(Sw)组成。砾石成分为灰岩和方解石。钻孔揭露周田组下伏地层厚度超

400 m, 岩性为石炭系黄龙组灰岩和白云岩, 为周田组地层提供了丰富的物源(廖达军等, 2019)。细砂岩中发育平行层理、脉状层理、低角度交错层理及板状交错层理, 表明了湖浪对滨岸带的反复冲刷; 泥质粉砂岩中可见波状和脉状层理, 也证实了这一结论。砂质层发育的虫迹, 表明滨湖带周期性的暴露于水面之上。

(2) 浅湖相。该沉积相主要有块状泥岩(Fm)和粉砂质泥岩(Fsm)组成, 夹少量薄层砂岩(Sp)。棕色泥岩和粉砂质泥岩的互层表明了浅湖相的沉积, 砂岩中平行和脉状层理的出现表明了较弱的水动力条件。

(3) 盐湖相。该沉积相主要有块状泥岩(Fm)、水平层理泥岩(Fh)和薄层石膏岩(Gp)组成, 夹少量构造破碎角砾岩(Gm)。泥岩和石膏岩频繁互层, 形成韵律层理。该沉积相以泥岩为主, 发育水平层理, 表明为湖水较浅的湖泊环境。同时, 发育的薄层状石膏岩, 表明在干旱气候下湖泊水体不断蒸干浓缩化学蒸发岩矿物从水体结晶沉淀形成, 指示了盐湖环境条件。

(4) 冲积-河流相、三角洲相。冲积-河流相主要有砾岩、含砾砂岩、砂岩和粉砂岩组成, 夹薄层泥岩(泰1井; 肖凯等, 2022)。地层底部发育厚层的砾岩、含砾砂岩; 中部由厚层砂岩和粉砂岩组成, 夹砾岩和泥岩薄层, 发育平行层理和波状层理; 上部主要由粉砂岩组成, 夹泥岩和砂岩, 发育水平层理和波状层理。三角洲相沉积主要由砂岩、粉砂岩和泥岩组成, 夹薄层砾岩, 发育水平层理、平行层理、波状层理、交错层理和韵律递变层理, 见冲刷构造、雨痕和虫迹(泰钾1井; 肖凯等, 2022)。

### 3.3 硫同位素特征

周田组石膏样品的硫同位素值( $\delta^{34}\text{S}_{\text{V-CDT}}$ )在8.0‰~15.4‰之间(表1), 主要集中在10.1‰~12.8‰之间。不同钻孔石膏硫同位素组成基本一致, 无明显差异。周田组石膏 $\delta^{34}\text{S}$ 值与新疆库车盆地渐新统石膏(10.1‰~13.3‰; 张华等, 2013)和罗布泊硫酸盐(7.4‰~11.5‰; 刘成林等, 1999)硫同位素值相似, 低于白垩纪时期海水硫同位素值(14‰~21‰; Strauss, 1999), 明显低于东濮凹陷、济阳坳陷、江陵凹陷和潜江凹陷古近系硫酸盐(26.1‰~40.4‰; 刘群等, 1987; 李任伟等, 1989; 史忠生等, 2005; 刘刚, 2007; 袁波等, 2008; 王春连等, 2013)及兰坪-思茅盆地上白垩统石膏(12.6‰~

表1 吉泰盆地周田组石膏硫同位素值 ‰

Table 1 Sulfur isotopic compositions of gypsums from the Zhoutian Formation of the Jitai Basin

样品编号	$\delta^{34}\text{S}_{\text{V-CDT}}$
ZK8001-1	14.4
ZK8001-2	14.1
ZK8001-3	10.1
ZK8001-4	8.2
ZK8001-5	8.3
M01-1	12.7
M01-2	12.2
M01-3	10.9
M02-1	10.8
M02-2	12.0
M02-3	14.8
M02-4	14.4
ZK8301-1	8.1
ZK8301-2	15.4
ZK8301-3	12.6
ZK8301-4	14.0
ZK8301-5	12.6
ZK8301-6	11.6
ZK8301-7	12.5
ZK8301-8	11.6
ZK8301-9	11.5
ZK8301-10	11.9
ZK8301-11	12.3
ZK8301-12	10.9
ZK8401-1	11.0
ZK8401-2	12.8
ZK8401-3	12.1
ZK8401-4	11.9

20.6‰; 刘群等, 1987; 王立成等, 2014)硫同位素值(图7)。

## 4 讨论

### 4.1 周田组沉积演化特征

根据梅岗地区钻孔岩芯岩相类型的识别和沉积相的划分, 周田组地层可分为下部的滨-浅湖相沉积和上部的咸水盐湖相沉积。周田组下段滨湖相岩性主要由砾岩、细砂岩和泥质粉砂岩组成。砾岩厚度大, 砾石成分大部分为灰岩。廖达军等(2019)根据钻孔岩芯揭露, 认为石炭统碳酸盐岩的风化为周田组提供了充足的物质来源。在湖浪对滨岸带的冲刷作用下, 砂质层中发育平行、脉状和波状层理以及低角度和板状交错层理。同时, 滨岸带常周期性暴露在水面之上, 细砂和粉砂层中发育生物潜穴足迹。浅湖相岩性以泥岩和粉砂质泥岩为主, 受水体扰动

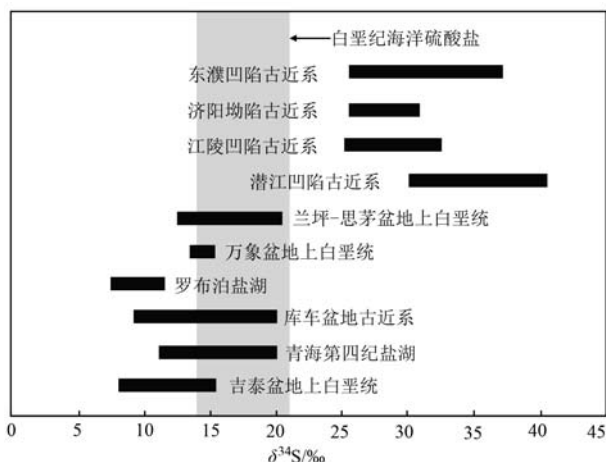


图7 不同蒸发岩盆地硫酸盐硫同位素组成

Fig. 7 Sulfur isotopic compositions of sulfate in different evaporite basins

白垩纪海洋硫酸盐数据来自 Strauss (1999)；东濮凹陷数据来自李任伟等(1989)和史忠生等(2005)；济阳坳陷数据来自袁波等(2008)；江陵凹陷数据来自王春连等(2013)；潜江凹陷数据来自刘群等(1987)和刘刚(2007)；兰坪-思茅盆地数据来自刘群等(1987)和王立成等(2014)；万象盆地数据来自张华等(2013)；罗布泊盐湖数据来自刘成林等(1999)；库车盆地数据未见(2013)；青海盐湖数据来自魏新俊等(1993)。

data of Cretaceous marine sulfate are from Strauss (1999); data of Dongpu Depression are from Li Renwei *et al.* (1989) and Shi Zhongsheng *et al.* (2005); data of Jiangling Depression are from Yuan Bo *et al.* (2008); data of Qianjiang Depression are from Wang Chunlian *et al.* (2013); data of Jianjiang Depression are from Liu Qun *et al.* (1987) and Liu Gang (2007); data of Lanping-Simao Basin are from Liu Qun *et al.* (1987) and Wang Licheng *et al.* (2014); data of Vientiane Basin are from Zhang Hua *et al.* (2014); data of Lop Nur salt lake are from Liu Chenglin *et al.* (1999); data of Kuqa Basin are from Zhang Hua *et al.* (2013); data of Qinghai salt lake are from Wei Xinjun *et al.* (1993).

相对较弱,粉砂质层中发育水平层理和脉状层理。周田组上段盐湖相沉积主要由泥岩和石膏岩组成,不同于上段的湖相碎屑岩沉积。化学蒸发岩的出现表明气候变干旱,蒸发量增强,水体不断蒸发浓缩。同时,受潮流作用影响,水平层理发育。泥岩和石膏岩韵律互层,表明了湖水盐度存在周期性的咸化和淡化转化过程。

#### 4.2 石膏硫同位素组成的地质意义

水体蒸发结晶过程中,硫同位素值分馏微弱,海水与海相硫酸盐硫同位素有相似的同位素组成(Holser and Kaplan, 1966; Strauss, 1999; Kampschulte and Strauss, 2004)。现代海水硫酸盐具有相

对稳定的  $\delta^{34}\text{S}$  值在  $19.3\text{‰} \sim 21.1\text{‰}$  之间,平均值约  $20.5\text{‰}$  (Strauss, 1999);由于沉积环境的波动,陆相湖盆中硫酸盐  $\delta^{34}\text{S}$  值变化较大(郑喜玉等, 1988; 史忠生等, 2005)。蒸发岩盆地内硫酸盐  $\delta^{34}\text{S}$  值主要受控于细菌硫酸盐还原作用和新水体的补给(Fry *et al.*, 1986; 史忠生等, 2005)。细菌硫酸盐还原作用导致最大的同位素分馏,可达  $50\text{‰} \sim 60\text{‰}$  (Fry *et al.*, 1986),其结果是硫酸盐  $\delta^{34}\text{S}$  值显著变大,而形成的硫化物同位素明显亏损(Strauss, 1997)。淡水富集轻的同位素 $^{32}\text{S}$ ,新水体的补给会导致硫酸盐的  $\delta^{34}\text{S}$  值降低(Makhnach *et al.*, 2000)。

中国东部裂谷系东濮凹陷、济阳坳陷、潜江凹陷和江陵凹陷古近系含盐层系硫酸盐具有较高的  $\delta^{34}\text{S}$  值,远高于同时期的海水硫同位素值( $17\text{‰} \sim 22\text{‰}$ ; Kampschulte and Strauss, 2004),这主要是硫酸盐细菌还原作用的结果。低的硫酸盐  $\delta^{34}\text{S}$  值,如新疆库车盆地渐新统石膏和罗布泊硫酸盐及西藏盐湖( $3.9\text{‰} \sim 6.9\text{‰}$ ),可能是湖盆在相对开放的地表环境受到周边淡水的补给。

吉泰盆地周田组石膏  $\delta^{34}\text{S}$  值为  $8.0\text{‰} \sim 15.4\text{‰}$ ,主要集中在  $10.1\text{‰} \sim 12.8\text{‰}$  之间,低于白垩纪海水硫同位素值( $14\text{‰} \sim 21\text{‰}$ ; Strauss, 1999),明显不同于硫酸盐细菌还原作用有关的硫同位素组成。这表明,吉泰盆地周田组石膏形成过程中,细菌还原作用微弱,对石膏硫同位素分馏贡献很小。盆地内含膏层系缺少黄铁矿等还原硫化物(图 4),进一步表明石膏形成过程中,成盐环境对硫酸盐来说是开放的。周田组石膏  $\delta^{34}\text{S}$  值的波动表明不同程度的淡水补给,可能与盆地物源的变化有关(史忠生等, 2005; 王立成等, 2014)。

#### 4.3 沉积模式

基于梅岗地区钻孔岩芯岩石类型和沉积相分析,结合前人对吉泰盆地上白垩统周田组沉积特征和演化研究资料,本次总结了吉泰盆地周田组沉积时期岩相古地理展布和沉积模式特征。

周田组沉积时期,吉泰盆地主体呈北东向展布,南深北浅、东深西浅的地形特征,碎屑物源主要来自北西和南东向造山带的剥露(卢秋芽, 1991; 肖凯等, 2022)。沉积岩相的分布受物源、古地貌和古气候控制。

周田组沉积早期,盆地南部和东部边界断层活跃,沉积中心位于盆地东部泰和与宜春地区之间(肖凯等, 2022)。前人研究表明(廖瑞君, 2000; 肖凯

等, 2022), 由于盆缘断层运动, 盆地物源补给量增加, 湖盆边缘物源区于田和苑前地区发育冲积-河流相沉积, 向盆地内过渡为三角洲相(图 8a)。湖盆沉积中心位于泰和与值夏地区, 发育滨-浅湖相(图 8a)。周田组沉积晚期, 气候逐渐变得干旱, 湖水不断蒸发浓缩形成了盐湖环境, 在梅岗地区发育泥岩和石膏岩的韵律沉积(图 8b)。

二维地震剖面构造解译揭示高陂-梅岗隆起、泰和凹陷和南部斜坡带基底呈现不对称的簸箕形状, 其中高陂-梅岗隆起内部发育正、逆断层, 导致微断裂发育, 周田组地层地震波组不连续, 表明其破碎严重(刘志伟等, 2022)。周田组发育构造角砾岩和硬石膏充填的裂隙也证实了断层活动活跃, 断裂带的发育为卤水提供了优质的储集体。石膏较低的 $\delta^{34}\text{S}$

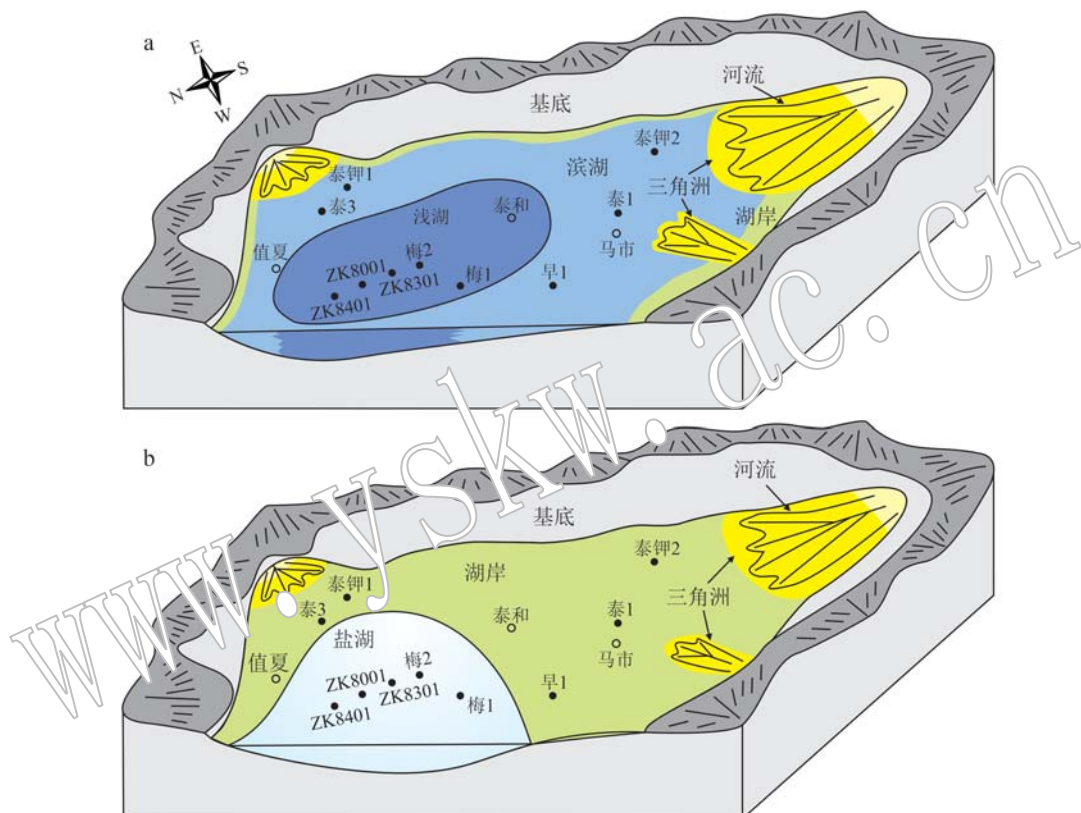


图 8 吉泰盆地周田组沉积模式图(据肖凯等, 2022 改编)

Fig. 8 Depositional model of the Zhoutian Formation of the Jitai Basin (adapted from Xiao Kai *et al.*, 2022)

a—周田组下段沉积期; b—周田组上段沉积期

a—sedimentary stage of the Lower Zhoutian Formation; b—sedimentary stage of the Upper Zhoutian Formation

值也指示该时期是一个开放的成盐环境。

#### 4.4 储层空间展布及远景分析

吉泰盆地梅岗地区周田组深层卤水主要赋存于破碎带储集体, 卤水层深度 148.80~254.07 m, 受地层压力的影响, 卤水具有承压性质(周敏娟等, 2017)。在储卤地层中, 岩心破碎, 角砾岩发育。在粉砂质条带及角砾岩中, 溶蚀孔洞发育。卤水层顶底板岩性为青灰色-紫红色含膏泥岩, 地层产状较缓; 微裂隙发育, 产状近直立, 石膏充填。

基于吉泰盆地泰和凹陷二维地震解译和钻孔资

料, 发现盆地深部发育 NE 走向、NW 倾向的正断层, 高陂-梅岗低隆起深部存在逆断层, 导致周田组微裂隙发育, 北西向深部可能存在富锂卤水矿床(刘志伟等, 2022)。根据周田组地层厚度和沉积模式特征(图 3、图 8), 梅岗地区含盐系地层向北西增厚, 并且构造裂隙、石膏充填的裂隙以及构造角砾岩更加发育。这些特征表明高陂-梅岗低隆起区西北凹陷可能是卤水储层的有利储集区, 显示了该区具有良好的卤水矿勘探潜力。同时, 含盐系地层发育的石膏和泥岩可作为盖层, 让卤水矿得以圈闭和保存。

## 5 结论

(1) 吉泰盆地东南部梅岗矿区的周田组下部为滨-浅湖相碎屑岩沉积,砂质岩中发育平行、脉状和波状层理以及低角度或板状交错层理,湖岸带细砂和粉砂层中发育潜穴足迹,具周期性暴露特点;周田组上部为盐湖相沉积,主要由泥岩和石膏岩韵律互层组成,水平层理发育,湖水盐度存在周期性的咸化和淡化转化过程。

(2) 周田组的石膏具有相对低的 $\delta^{34}\text{S}$ 值(8.0‰~15.4‰),表明石膏沉积过程中细菌还原作用微弱,形成于开放的成盐环境。

(3) 周田组沉积早期,气候湿润,物源补给量增加,盆缘物源区在于田和苑前地区发育冲积-河流相沉积,向盆地内过渡为三角洲相,湖盆中心为滨-浅湖相;周田组沉积晚期,气候变干旱,为湖水不断蒸发现浓缩的盐湖环境。构造角砾岩和硬石膏充填的裂隙发育表明构造活动活跃,断裂带的发育为卤水提供了优质的储集体。

(4) 梅岗地区含盐系地层向西北变厚,裂隙储集体发育,高陂-梅岗低隆起区西北凹陷是有利的卤水储集区,具有良好的找矿勘探潜力。含盐系地层发育的石膏和氯盐作为盖层,为富锂卤水的圈闭和保存起到重要作用。

**致谢** 野外工作得到江西省地质局第五地质大队李强高工、吴强工程师的大力支持,审稿专家提出许多建设性的意见,大大地提升了论文质量,在此一并致谢!

## References

- Bradley D, Munk L A, Jochens H, et al. 2013. A preliminary deposits model for lithium brines [R]. USGS, Open-file-2013-1006.
- Bureau of Geology and Mineral Resources of Jiangxi Province. 1997. Rock Stratigraphy in Jiangxi Province [M]. Wuhan: China University of Geosciences Press (in Chinese).
- Chen L Q, Steel R J, Guo F S, et al. 2017. Alluvial fan facies of the Yongchong Basin: Implications for tectonic and paleoclimatic changes during Late Cretaceous in SE China [J]. Journal of Asia Earth Sciences, 134: 37~54.
- Chen Piji. 1997. Coastal mountains of SE China, desertization and saliniferous lakes of Central China during the Late Cretaceous [J]. Journal of Stratigraphy, 21(3): 203~213 (in Chinese with English abstract).
- Dugamin E J M, Richard A, Cathelineau M, et al. 2021. Groundwater in sedimentary basins as potential lithium resource: A global prospective study [J]. Scientific Reports, 11: 21091.
- Fry B, Cox J, Gest H, et al. 1986. Discrimination between  $^{34}\text{S}$  and  $^{32}\text{S}$  during bacterial metabolism of inorganic sulfur compounds [J]. Journal of Bacteriology, 165(1): 328~330.
- Gilder S, Keller G R, Ming L, et al. 1991. Eastern Asia and the Western Pacific timing and spatial distribution of rifting in China [J]. Tectonophysics, 197: 225~243.
- Holser W T and Kaplan I R. 1966. Isotope geochemistry of sedimentary sulfates [J]. Chemical Geology, 1: 93~135.
- Jiang Xinsheng and Li Yuwen. 1996. Spatio-temporal distribution of the cretaceous deserts in central and eastern China and its climatic significance [J]. Sedimentary Facies and Palaeogeography, 16(2): 42~51 (in Chinese with English abstract).
- Jing X, Pan Z X, Xu J S, et al. 2008. Late Cretaceous Aeolian dunes and reconstruction of palaeowind belts of the Xinjiang Basin, Jiangxi Province, China [J]. Palaeogeography, Palaeoclimatology, Palaeoecology, 257: 58~66.
- Kampschulte A and Strauss H. 2004. The sulfur isotopic evolution of Phanerozoic seawater based on the analysis of structurally substituted sulfate in carbonates [J]. Chemical Geology, 204: 255~286.
- Li J H, Zhang Y Q, Dong S W, et al. 2014. Cretaceous tectonic evolution of South China: A preliminary synthesis [J]. Earth-Science Reviews, 56: 1 602~1 629.
- Li Q K, Fan Q S, Wang J P, et al. 2019. Hydrochemistry and distribution and formation of lithium-rich brines in salt lake on the Qinghai-Tibetan Plateau [J]. Minerals, 9: 528.
- Li Renwei and Xin Maoan. 1989. Origin of evaporites of Dongpu Basin [J]. Acta Sedimentologica Sinica, 7(4): 141~147 (in Chinese with English abstract).
- Liao Dajun, Ouyang Bin, Zhang Dongliang, et al. 2019. Preliminary study on the ore-forming geological background of lithium brine in Taihe Sag, Jitai Basin, Jiangxi Province [J]. World Nonferrous Metals, (23): 178~179 (in Chinese with English abstract).
- Liao Ruijun. 2000. Study on sedimentary deposits in the red continental basin of Ji'an-Taihe, Jiangxi [J]. Regional Geology of China, 19(2): 181~186 (in Chinese with English abstract).
- Liu Chenglin, Wang Mili and Jiao Pengcheng. 1999. Hydrogen, oxygen, strontium and sulfur isotopic geochemistry and potash forming material

- sources of Lop salt lake, Xinjiang [J]. *Mineral Deposits*, 18(3): 268~275 (in Chinese with English abstract).
- Liu Chenglin, Yu Xiaocan, Zhao Yanjun, et al. 2016. A tentative discussion on regional metallogenic background and mineralization mechanism of subterranean brines rich in potassium and lithium in South China Block [J]. *Mineral Deposits*, 35(6): 1119~1143 (in Chinese with English abstract).
- Liu Gang. 2007. The application of geochemical analysis to the study of sedimentary environment of Qianjiang Formation in Qianjiang Depression [J]. *Acta Geoscientica Sinica*, 28(4): 335~340 (in Chinese with English abstract).
- Liu Qun, Chen Yuhua, Li Yincai, et al. 1987. Mesozoic-Cenozoic Tertiary Clastic-chemical Rock Salt Deposits in China [M]. Beijing: Science and Technology Press (in Chinese).
- Liu Zhiwei, Hou Xianhua, Zheng Mianping, et al. 2022. Deep structural characteristics of depressional basin with lithium (potash)-rich brines: An example of Jitai Basin in South China [J]. *Earth Science*, 47(1): 110~121 (in Chinese with English abstract).
- López-Steinmetz R L and Salvi S. 2021. Brine grades in Andean salars: When basin size matters a review of the lithium triangle [J]. *Earth Science Reviews*, 217: 103615.
- López-Steinmetz R L, Salvi S, Schi C, et al. 2020. Lithium and brine geochemistry in the salars of the southern Puna Andean Plateau of Argentina [J]. *Economic Geology*, 115: 1079~1096.
- Lu Qiuya. 1991. Characteristics of Cretaceous sedimentation in Taihe Depression, Jitai Basin, Jiangxi Province [J]. *Geophysical & Geochemical Exploration*, 15(5): 395~398 (in Chinese with English abstract).
- Luo Huiping, Zhu Jun and Li Bo. 2018. Geological characteristics and genesis of the Meigang rich lithium brine mine in Jitai Basin, Jiangxi Province [J]. *World Nonferrous Metals*, (20): 205~206 (in Chinese with English abstract).
- Ma Houming, Lai Zhijian, Yan Xinhua, et al. 2021. Geochemical characteristics and prospect analysis of brine lithium deposits in Jitai Basin, Jiangxi Province [J]. *Acta Geoscientica Sinica*, 42(5): 617~627 (in Chinese with English abstract).
- Makhnach A, Mikhajlov N, Kolosov I, et al. 2000. Comparative analysis of sulfur isotope behavior in the basins with evaporites of chloride and sulfate types [J]. *Sedimentary Geology*, 134: 343~360.
- Munk L A, Hynek S A, Bradley D C, et al. 2016. Lithium brines: A global perspective [J]. *Reviews in Economic Geology*, 18: 339~365.
- Peng Touping, Wang Yuejun, Jiang Zhimin, et al. 2004.  $^{40}\text{Ar}/^{39}\text{Ar}$  geochronology and geochemistry of Cretaceous basaltic rocks for the central and northwestern Jiangxi Province [J]. *Geochimica*, 33(5): 447~458 (in Chinese with English abstract).
- Shi Zhongsheng, Chen Kaiyuan and He Sheng. 2005. Strontium, sulfur and oxygen isotopic compositions and significance of paleoenvironment of Paleogene of Dongpu Depression [J]. *Acta Geoscientica Sinica*, 30(6): 430~436 (in Chinese with English abstract).
- Shu L S, Zhou X M, Deng P, et al. 2009. Mesozoic tectonic evolution of the Southeast China Block: New insights from basin analysis [J]. *Journal of Asian Earth Sciences*, 34: 376~391.
- Strauss H. 1997. The isotopic composition of sedimentary sulfur through time [J]. *Palaeogeography, Palaeoclimatology, Palaeoecology*, 132: 97~118.
- Strauss H. 1999. Geological evolution from isotope proxy signals-sulfur [J]. *Chemical Geology*, 161: 89~91.
- Wang Chunlian, Liu Chenglin, Xu Haiming, et al. 2013. Sulfur isotopic composition of sulfate and its geological significance of Member 4 of Paleocene Jitai Formation in Jiangling Depression of Hubei Province [J]. *Journal of Jilin University: Earth Science Edition*, 43(3): 691~703 (in Chinese with English abstract).
- Wang Chunlian, Liu Lihong, Li Qiang, et al. 2020. Petrogeochemical characteristics and genetic analysis of the source area of brine type lithium-potassium ore sources area in Jitai basin of Jiangxi Province [J]. *Acta Petrologica et Mineralogica*, 39(1): 65~84 (in Chinese with English abstract).
- Wang Jiuyi, Liu Chenglin, Wang Chunlian, et al. 2021. Tectono-paleoclimatic coupling process for mineralization of Late Cretaceous-Paleogene evaporites in South China [J]. *Acta Geologica Sinica*, 95(7): 2041~2051 (in Chinese with English abstract).
- Wang Licheng, Liu Chenglin, Fei Mingming, et al. 2014. Sulfur isotopic composition of sulfate and its geological significance of the Yunlong Formation in the Lanping Basin, Yunnan Province [J]. *China Mining Magazine*, 23(12): 57~64 (in Chinese with English abstract).
- Warren J K. 2010. Evaporites through time: Tectonic, climatic and eustatic controls in marine and nonmarine deposits [J]. *Earth-Science Reviews*, 98: 217~268.
- Wei Xinjun, Shao Changduo, Zhao Dejun, et al. 1993. Study on Material Composition, Sedimentary Characteristics and Forming Conditions of Potassium-rich Salt Lakes in Western Qaidam Basin [M]. Beijing: Geological Publishing House, 70~71 (in Chinese with English abstract).
- Xiao Kai, Xiong Kai, Gao Zhaowei, et al. 2022. Tectono-sedimentary characteristics and analysis of evolution of the Jitai Basin [J]. *Mineral*

- Exploration, 13(11): 1 603~1 611 (in Chinese with English abstract).
- Xiao Zeyou, Qi Fuyong, Fan Huihu, et al. 2023. Geological characteristics and prospecting potential of brine-type lithium ores in Ganzhou Basin, Jiangxi Province [J]. East China Geology, 44(4): 367~375 (in Chinese with English abstract).
- Xu W J and Xu X S. 2015. Early Paleozoic intracontinental felsic magmatism in the South China Block: Petrogenesis and geodynamics [J]. Lithos, 234~235: 79~92.
- Yan Y, Hu X Q, Lin G, et al. 2011. Sedimentary provenance of the Hengyang and Mayang basins, SE China, and implications for the Mesozoic topographic change in South China Craton: Evidence from detrital zircons geochronology [J]. Journal of Asia Earth Sciences, 41: 494~503.
- Yu X C, Liu C L, Wang C L, et al. 2021. Late Cretaceous aeolian desert system within the Mesozoic fold belt of South China: Palaeoclimatic changes and tectonic forcing of East Asian erg development and preservation [J]. Palaeogeography, Palaeoclimatology, Palaeoecology, 567: 110299.
- Yu Xiaocan, Liu Chenglin, Wang Chunlian, et al. 2022. Genesis of lithium brine deposits in the Jianghan Basin and progress in resource exploration: A review [J]. Earth Science Frontiers, 29(1): 107~123 (in Chinese with English abstract).
- Yu X C, Liu C L, Wang C L, et al. 2022. Origin of Li brine-type deposits in the eolian gypsum-bearing formation of the Jitai basin, South China: Constraints from geochemistry and H, O, Li, B, and Sr isotopes [J]. Applied Geochemistry, 139: 105257.
- Yu Xinqi, Shu Liangshu, Deng Guohui, et al. 2005. Geochemical features and tectonic significance of the alkali basalts from Ji'an-Taihe Basin, Jiangxi Province [J]. Geoscience, 19(1): 133~140 (in Chinese with English abstract).
- Yuan Bo, Chen Shiyue, Yuan Wenfang, et al. 2008. Characteristics of strontium and sulfur isotopes in Shahejie Formation of Jiayang Depression [J]. Journal of Jilin University: Earth Science Edition, 38(4): 613~617 (in Chinese with English abstract).
- Zhang Hua, Liu Chenglin, Cao Yangtong, et al. 2013. A tentative discussion on the time and the way of marine regression from Tarim Bay during the Cenozoic [J]. Acta Geoscientica Sinica, 34(5): 577~584 (in Chinese with English abstract).
- Zhang Hua, Liu Chenglin, Wang Licheng, et al. 2013. Characteristics of evaporites sulfur isotope from potash deposit in Thakhek Basin, Laos, and its implication for potash formation [J]. Geological Review, 60(4): 851~857 (in Chinese with English abstract).
- Zhang Xiying, Shan Fashou, Shi Guocheng, et al. 2016. Distribution characteristics of main ore-forming elements in brines of salt lakes and comprehensive evaluation of resource endowment for these elements in China [J]. Journal of Salt Lake Research, 24(2): 1~11 (in Chinese with English abstract).
- Zheng Xiyu, Tang Yuan and Xu Chang. 1988. Tibet Saline Lake [M]. Beijing: Science and Technology Press (in Chinese).
- Zhou Minjuan, Hu Li, Huang Xiaonian, et al. 2017. Metallogenic geological characteristics and prospect of development and utilization of Meigang Li-bearing brine deposit in Taihe County, Jiangxi Province [J]. Modern Mining, 33(11): 61~64 (in Chinese with English abstract).
- Zhou X M and Li W X. 2000. Origin of Late Paleozoic igneous rocks in Southeastern China: Implications for lithospheric subduction and underplating of mafic magmas [J]. Tectonophysics, 326: 269~287.
- Zhou X M, Sun Y, Shen W Z, et al. 2006. Petrogenesis of Mesozoic granitoids and volcanic rocks in South China: A response to tectonic evolution [J]. Episodes, 29: 26~33.
- Zhong Mingbo, Wu Zhongru, Wang Sixue, et al. 2022. Geological characteristics and genesis of Nanzhou lithium brine deposit in Jitai basin, Jiangxi Province [J]. Resources Environment & Engineering, 36(2): 142~148 (in Chinese with English abstract).
- ## 附中文参考文献
- 陈丕基. 1997. 晚白垩世中国东南沿岸山系与中南地区的沙漠和盐湖化 [J]. 地层学杂志, 21(3): 203~213.
- 江西省地质矿产局. 1997. 江西省岩石地层 [M]. 武汉: 中国地质大学出版社.
- 江新胜, 李玉文. 1996. 中国中东部白垩纪沙漠的时空分布及其气候意义 [J]. 岩相古地理, 16(2): 42~51.
- 李任伟, 辛茂安. 1989. 东濮盆地蒸发岩成因 [J]. 沉积学报, 7(4): 141~147.
- 廖达军, 欧阳斌, 张栋梁, 等. 2019. 江西省吉泰盆地泰和凹陷含锂卤水矿成矿地质背景初步研究 [J]. 世界有色金属, (23): 178~179.
- 廖瑞君. 2000. 江西吉安-泰和陆相红色盆地沉积体研究 [J]. 中国区域地质, 19(2): 181~186.
- 刘成林, 王弭力, 焦鹏程. 1999. 新疆罗布泊盐湖氯氧锶同位素地球化学及钾矿成矿物质来源 [J]. 矿床地质, 18(3): 268~275.
- 刘成林, 余小灿, 赵艳军, 等. 2016. 华南陆块液体钾锂资源的区域成矿背景与成矿作用初探 [J]. 矿床地质, 35(6): 1119~1143.

- 刘刚. 2007. 运用地球化学分析研究潜江凹陷潜江组沉积环境[J]. 地球学报, 28(4): 335~340.
- 刘群, 陈郁华, 李银彩, 等. 1987. 中国中、新生代陆源碎屑-化学岩型盐类沉积[M]. 北京: 科学技术出版社.
- 刘志伟, 侯献华, 郑绵平, 等. 2022. 含富锂(钾)卤水断陷盆地的深部构造特征: 以中国华南吉泰盆地为例[J]. 地球科学, 47(1): 110~121.
- 卢秋芽. 1991. 江西吉泰盆地泰和坳陷白垩纪沉积特征[J]. 物探与化探, 15(5): 395~398.
- 罗辉平, 朱俊, 李波. 2018. 江西吉泰盆地梅岗富锂卤水矿地质特征及成因[J]. 世界有色金属, (20): 205~206.
- 马厚明, 赖志坚, 鄢新华, 等. 2021. 江西吉泰盆地卤水锂矿床地球化学特征及远景分析[J]. 地球学报, 42(5): 617~627.
- 彭头平, 王岳军, 江志敏, 等. 2004. 江西中西部地区白垩纪玄武质岩石的<sup>40</sup>Ar/<sup>39</sup>Ar年代学和地球化学研究[J]. 地球化学, 33(5): 447~458.
- 史忠生, 陈开远, 何生. 2005. 东濮盐湖古近系锶、硫、氧同位素组成及古环境意义[J]. 地球学报, 30(6): 430~436.
- 王春连, 刘成林, 徐海明, 等. 2013. 湖北江陵凹陷古新统沙市组四段硫酸盐硫同位素组成及其地质意义[J]. 吉林大学学报: 地球科学版, 43(3): 691~703.
- 王春连, 刘丽红, 李强, 等. 2020. 江西吉泰盆地卤水型锂钾矿物源区岩石地球化学特征及成因分析[J]. 岩石矿物学杂志, 39(1): 6~11.
- 王九一, 刘成林, 王春连, 等. 2021. 晚白垩世-古近纪华南蒸发岩矿床形成的构造和气候耦合控制[J]. 地质学报, 95(7): 2041~2051.
- 王立成, 刘成林, 费明月, 等. 2014. 云南兰坪盆地云龙组硫酸盐硫同位素特征及其地质意义[J]. 中国矿业, 23(12): 57~64.
- 魏新俊, 邵长锋, 赵德钧, 等. 1993. 柴达木盆地西部富钾盐湖物质组分、沉积特征及形成条件研究[M]. 北京: 地质出版社, 70~71.
- 肖凯, 熊凯, 高赵伟, 等. 2022. 吉泰盆地构造沉积特征及演化分析[J]. 矿产勘查, 13(11): 1603~1611.
- 肖则佑, 漆富勇, 范会虎, 等. 2023. 江西赣州盆地盐湖型锂矿地质特征及找矿前景[J]. 华东地质, 44(4): 367~375.
- 余小灿, 刘成林, 王春连, 等. 2022. 江汉盆地大型富锂卤水矿床成因与资源勘查进展: 综述[J]. 地学前缘, 29(1): 107~123.
- 余心起, 舒良树, 邓国辉, 等. 2005. 江西吉泰盆地碱性玄武岩的地球化学特征及构造意义[J]. 现代地质, 19(1): 133~140.
- 袁波, 陈世悦, 袁文芳, 等. 2008. 济阳坳陷沙河街组锶同位素特征[J]. 吉林大学学报: 地球科学版, 38(4): 613~617.
- 张华, 刘成林, 曹养同, 等. 2013. 大里木古海湾新生代海退时限及方式的初步探讨[J]. 地球学报, 34(5): 577~584.
- 张华, 刘成林, 王立成, 等. 2014. 老挝他曲盆地钾盐矿床蒸发岩硫同位素特征及成钾指示意义[J]. 地质论评, 60(4): 851~859.
- 张西营, 山发寿, 石国成, 等. 2016. 中国盐湖卤水主要成矿元素分布特征及其资源禀赋综合评价[J]. 盐湖研究, 24(2): 1~11.
- 郑喜玉, 唐渊, 徐昶. 1988. 西藏盐湖[M]. 北京: 科学技术出版社.
- 周敏娟, 胡立, 黄小年, 等. 2017. 江西省泰和县梅岗含锂卤水矿成矿地质特征及开发利用前景[J]. 现代矿业, 33(11): 61~64.
- 朱明波, 吴忠如, 王思学, 等. 2022. 江西省吉泰盆地南洲含锂卤水矿床地质特征及成因探讨[J]. 资源环境与工程, 36(2): 142~148.